Table 2 Convergence of the Fourier series

Order of the series	6	10	20
A_3/A_1	8.418E−03	8.418E−03	8.418E−03
A_5/A_1	7.818E−04	7.831E−04	7.831E−04
A_7/A_1	—	1.853E−04	1.853E−04
A_9/A_1	—	6.516E−05	6.528E−05
A_{11}/A_1	—	—	2.870E−05
A_{13}/A_1	—	—	1.455E−05
A_{15}/A_1	—	—	8.149E−06
A_{17}/A_1	—	—	4.916E−06
A_{19}/A_1	—	—	3.136E−06

Table 3 Effect of aspect ratio on the optimum drag

Aspect ratio	Total drag coefficient (elliptic)	Total drag coefficient (optimum)
5	0.07638	0.07637
10	0.04455	0.04453
15	0.03394	0.03391
20	0.02863	0.02860
25	0.02545	0.02540
30	0.02333	0.02327

In the above example, a total of six terms was used in the Fourier series. Table 2 shows the convergence rate of the series for larger number of terms. It is quite evident from this table that the resulting series converges quite rapidly. The drag coefficients corresponding to the different cases presented in this table were identical.

The above example employed a wing with an aspect ratio of 6. As the aspect ratio changes, so would the relative significance of the induced drag and the viscous drag. Therefore, the problem was solved over a range of aspect ratios. The results are shown in Table 3. As expected, increasing the aspect ratio decreases the induced drag, increasing the significance of the viscous drag. This suggests that for high aspect ratio wings such as those on sail planes, the twist should perhaps be optimized for least total drag.

In all of the above cases, judging from the magnitude of the numbers, optimization for viscous drag does not appear to pay off. In every case, any reduction in viscous drag was nearly offset by a corresponding increase in induced drag. Even for large aspect ratio cases, where the induced drag tends to lose its dominance, the same gain in total drag can be realized by slightly increasing the aspect ratio. Furthermore, it is quite evident, that the base drag [i.e., 0.0058 in Eq. (9)] is the dominant part of viscous drag. So any effort in reducing the viscous drag should be concentrated on reducing this value.

Conclusions

It was demonstrated how the classical lifting line theory can be modified for the effect of viscous drag. The governing equations were developed and applied to a rectangular wing. The airfoil chosen for this example resembled NACA-0012 at Reynolds number of three million. Rapid convergence of the resulting series was demonstrated. It was shown that the inclusion of viscous drag indeed renders the elliptic lift distribution nonoptimal. However, in every case, the reduction in viscous drag was very closely matched by an increase in induced drag. Therefore, the reduction in total drag, within the confines of this theory, was determined to be negligible. Nonetheless, this exercise raises the possibility of employing similar techniques in conjunction with vortex lattice or panel methods.

References

[1]Prandtl, L, *Applied Hydro and Aeromechanics*, McGraw-Hill, New York, 1957.

[2]Loth, J. L, and Boyle, R. E., "Optimum Loading on Nonplanar Wings at Minimum Induced Drag," NASA Rept. AD-704502, Aug. 1969.

[3]Lundry, J. L., "A Numerical Solution for the Minimum Induced Drag, and Corresponding Loading, of Nonplanar Wings," NASA CR-1218, Nov. 1968.

[4]Lamar, J. E., "A Modified Multhopp Approach for Predicting Lifting Pressures and Camber Shape for Composite Planforms in Subsonic Flow," NASA TN-D-4427, July 1968.

[5]Moran, J., *An Introduction to Theoretical and Computational Aerodynamics*, Wiley, New York, 1984.

[6]Kuethe, A. M., and Chow, C.-Y., *Foundations of Aerodynamics*, 3rd ed., Wiley, New York, 1976.

[7]Abbott, I. H., and von Doenhoff, A. E., *Theory of Wing Sections*, Dover, New York, 1959.

PAN AIR Analysis of Simply Connected Control Surface Deflections

Seth A. Moyer*
Naval Air Warfare Center,
Warminster, Pennsylvania 18974

Nomenclature

FS, WL, BL	=	aircraft fuselage station, waterline, buttline, in.
M_∞	=	freestream Mach number
n	=	upper surface unit normal
W	=	total mass flux
α, A	=	aircraft angle of attack, deg
α_{xz}, α_{xy}	=	local flowfield angle of upwash and sidewash, deg
β	=	nondimensional mass flux magnitude
Θ	=	flap deflection angle, deg positive down

Introduction

SEVERAL existing and planned fighter/attack aircraft have control surface deflection schedules that are dependent upon flight condition. Effective flowfield analysis of these aircraft must include proper modeling of leading- and trailing-edge flap effects. This is particularly important in store carriage and release analysis where a store is oriented such that there is significant interaction between the flap and store surfaces.

The present study analyzes PAN AIR flap modeling of simply connected control surfaces. Simply connected control surfaces are those surfaces that move with pure rotation, or systems that approximate pure rotation. A modeling method based on proper specification of the boundary condition, as suggested in Ref. 2, is compared to several geometric approaches based on previous studies of more complex configurations. It is demonstrated that the representation of simply connected flap deflections by boundary condition specification is both accurate and efficient.

Background

PAN AIR[1–4] has proven useful in the past for predicting the aircraft-induced flowfield for complex aircraft configurations where flap deflections are not present.[5,6] Several studies have also been conducted on flap configurations using various "exact" approaches for modeling the deflections with PAN AIR.[7] These studies have been centered on complex

Received Feb. 12, 1992; revision received March 23, 1992; accepted for publication March 26, 1992.

*Aerospace Engineer, Aircraft Division. Member AIAA.

flap systems where flap rotation is combined with flap extension or full span surface deflections.

For small deflection angles, these complex systems approximate simply connected surfaces and have been modeled by integrating the flaps into the wing paneling. This technique insures doublet strength continuity in the chordwise direction. Semispan trailing-edge flap systems of this type introduce spanwise discontinuities that need to be accounted for. In one method these gaps have been filled by impermeable panels, creating a continuous trailing edge.[7] This approach was one method investigated in the present study. For larger deflections, the configuration no longer approximates a simply connected surface and a multiple element airfoil problem must be analyzed.

These and other methods proposed for studying flap deflections with PAN AIR require significant repaneling for each individual configuration and introduce complexities unnecessary for simply connected flaps. Furthermore, these methods may often set up panel models that have adjacent panels in close opposition or have panels of extremely small area with respect to adjacent panels. These situations may introduce significant numerical difficulties in the solutions.

Approach

Baseline Configuration

The basis for this study was the F/A-18 which exhibits flaps fitting the criteria of simple connected flaps. A baseline configuration was generated with flaps in the neutral position (leading edge = 0 deg, trailing edge = 0 deg) and network breaks coincident with control surface edges. This model was compared to wind-tunnel probe flowfield data to verify an accurate baseline model. Figure 1 presents a comparison of the flowfields for this model to the experimental data for $M_\infty = 0.8$, $\alpha = 0.0$. As indicated, the traverse was between FS 300 and 650 at WL = 62.5 and BL = 134.28 (under the outboard pylon). PAN AIR generates a flowfield that is in close agreement to the test data, as was previously demonstrated in Ref. 5.

Flap Configurations

Flap deflections were modeled by three geometric approaches and a boundary condition approach applied to the baseline model. The four methods were compared to each other based on PAN AIR flowfield solutions and the experimental data. A flap combination of 3-deg leading-edge down and 4-deg trailing-edge down was chosen for this study.

The difficulty in modeling the physical situation occurs in accounting for the spanwise discontinuities that occur between the lex/flap and flap/aileron when the flaps are deflected. When paneled physically, the discontinuity must be modeled such that the doublet strength is continuous over the discontinuity. The four approaches used in this study are illustrated in Fig. 2, using the trailing-edge flap/aileron discontinuity as an example.

The study was initiated with the most physically representative panel model as shown in Fig. 2a (end caps), with a spanwise gap between points B and C. The upper and lower flap surfaces were joined by surface end caps (as with wing tips) connecting points A-B-D and points A-C-D. The spanwise discontinuity between the two surfaces, A-B-C and D-B-C, were joined by wake panels. The next approach (Fig. 2b, thin edge) eliminated the end caps by transitioning the flap thickness to zero in the panels immediately adjacent to the discontinuity. Points A and D then collapse and the gap A/D-B-C is connected by a wake network. The third approach (Fig. 2c, solid te) again eliminated the need for end caps but maintains flap thickness by connecting the discontinuities A-B-C and D-B-C with a solid (impermeable) surface top and bottom, forming a continuous trailing edge (the method of Ref. 7).

The fourth approach requires no change to the undeflected geometry (B and C coincident) but utilizes a PAN AIR boundary condition permitting mass flux through a network panel.[2,3] The general boundary condition equation states that a specified mass flux, normal to the surface, is equal to the normal component of the total mass flux. For an impermeable surface this is represented by

$$W \cdot n = 0$$

However, for the specified mass flux boundary condition this becomes

$$W \cdot n = \beta$$

where β is the nondimensional mass flux magnitude along n. The sign of β is related to n such that flow into the panel is $-\beta$ and flow out is $+\beta$ as shown in Fig. 2d. This approach may be used to simulate the flow turning effect of the flap by specifying β to be $-\tan\Theta$ on the upper surface (flow in) and specifying β to be $+\tan\Theta$ on the lower surface (flow out), where Θ is the flap deflection angle.

Results

The comparison of the various approaches illustrated in Fig. 3 was conducted under the outboard pylon at $M_\infty = 0.8$, α

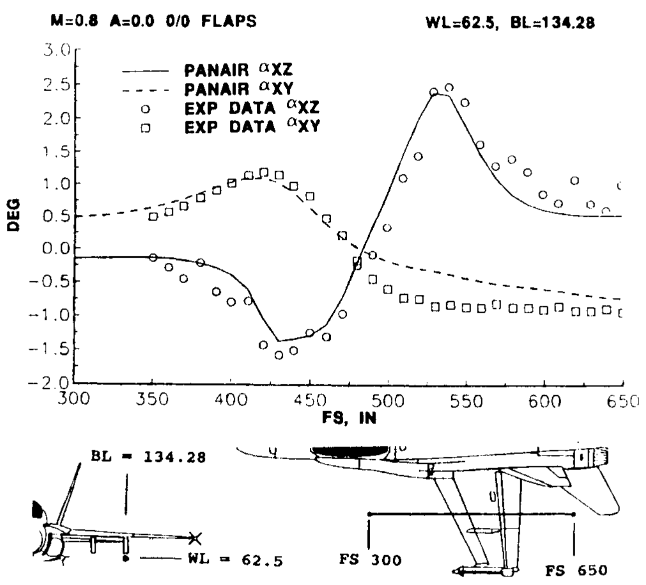

Fig. 1 Baseline flowfield comparison.

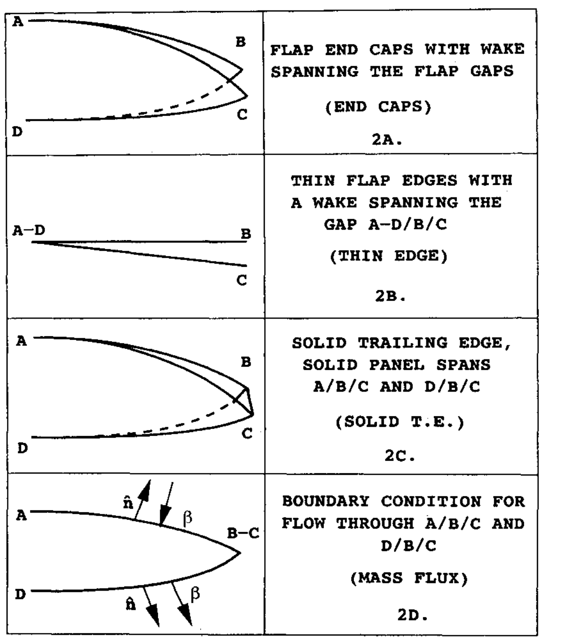

Fig. 2 Modeling approaches.

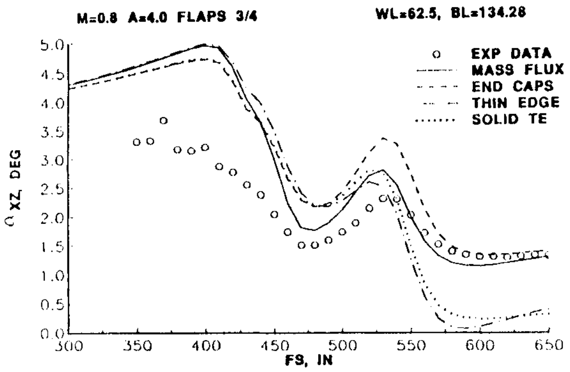

a) Upwash

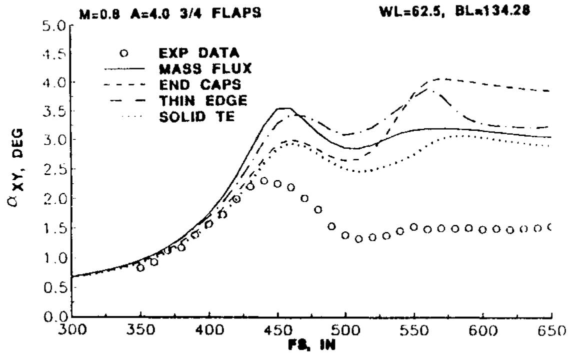

b) Sidewash

Fig. 3 Flowfield comparison of methods.

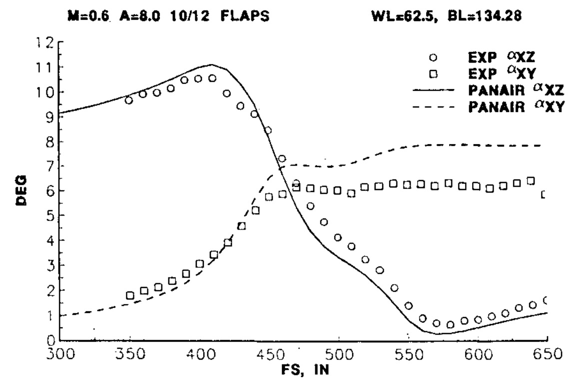

Fig. 4 Mass flux model, case 2.

= 4.0, for a flap deflection of 3-deg leading-edge down and 4-deg trailing-edge down. The inability of the first approach to accurately predict the sidewash flowfield led to the investigation of the other methods. Figure 3a is a comparison of the predicted upwash flowfield for the four methods with experimental data. It can be seen that the boundary condition method best models the upwash flowfield. Figure 3b presents the same comparison for the sidewash flowfield. For this particular flight condition and flap setting, none of the approaches accurately predict the sidewash very well. However, the boundary condition method fares as well as the other methods. The failure of the other methods to model the flowfield is more likely due to the numerical difficulties present in the solution, due to the discontinuity panels, than a failure in the physical modeling. In any event, it is clear that the mass flux specification performs adequately in predicting the flowfield, especially given its simplicity.

Due to the relatively good performance of the boundary condition approach and its ease of application, other conditions were investigated using just this method. Figure 4 presents the flowfield comparisons for $M_\infty = 0.6$, $\alpha = 8.0$, with 10/12 flaps. Again the only discrepancies appear in sidewash.

Conclusions

Several approaches to modeling simply connected flaps with PAN AIR have been investigated. The boundary condition method specifies mass flux through the flap to approximate the turning angle induced by the flap. Each method was compared to the other methods and to experimental data based on the flowfield directly under the outboard pylon.

Relative to the geometric approaches, the boundary condition approach does a very good job of modeling the upwash and sidewash flowfields. In absolute terms, compared to experimental data, this approach matches upwash well and sidewash to various levels, depending on flight condition. The attractive feature of this method is that it requires no geometry changes to a properly peneled baseline model in order to model flap settings. Analysis of many different flap configurations therefore becomes possible in a short time period. This method should apply equally as well to elevator and rudder deflection analysis. Due to its simplicity and accuracy, the boundary condition method of simply connected flap modeling provides an excellent tool for flowfield analysis.

References

[1]Magnus, A. E., and Epton, M. A., "PAN AIR—A Computer Program for Predicting Subsonic or Supersonic Linear Potential Flows About Arbitrary Configurations Using a Higher Order Panel Method, Vol. 1, Theory Document (Version 1.0)," NASA-CR-3251, 1980.

[2]Sidwell, K. W., Baruah, P. K., and Bussoletti, J. E., "PAN AIR—A Computer Program for Predicting Subsonic or Supersonic Linear Potential Flows About Arbitrary Configurations Using a Higher Order Panel Method, Vol. 2, User's Manual (Version 1.0)," NASA-CR-3252, 1980.

[3]Saaris, G. R., "A502H User's Manual—PAN AIR Technology Program for Solving Problems of Potential Flow About Arbitrary Configurations," Boeing Document D6-54703, Feb. 1990.

[4]Carmichael, R. L., and Erickson, L. L. "PAN AIR—A Higher Order Panel Method for Predicting Subsonic or Supersonic Linear Potential Flows About Arbitrary Configurations," AIAA Paper 81-1255, June 1981.

[5]Cenko, A., Tseng, W., and Madson, M., "Potential Flow Applications to Complex Configurations," AIAA Paper 91-1634, June 1991.

[6]Cenko, A., and Tessitore, F., "Evaluation of Methods for Predicting Complex Aircraft Flowfields," *Journal of Aircraft*, Vol. 25, No. 5, 1988, pp. 453–458.

[7]Tinoco, E. N., Ball, D. N., and Rice, F. A. II, "PAN AIR Analysis of a Transport High-Lift Configuration," *Journal of Aircraft*, Vol. 24, No. 3, 1987, pp. 181–187.

Lightning Threat to Aircraft: Do We Know All We Need to Know?

Vladislav Mazur*
NOAA/National Severe Storms Laboratory, Norman, Oklahoma 73069

Introduction

THE problem of lightning threat to aircraft has two aspects: 1) strike avoidance, and 2) aircraft protection. Let us address these two issues separately.

Received Oct. 16, 1991; revision received April 21, 1992; accepted for publication May 1, 1992.

*Physicist, Storm Electricity and Cloud Physics Group.